EROSIVE AUGMENTATION OF SOLID PROPELLANT BURNING RATE: MOTOR SIZE SCALING EFFECT*

L. D. Strand
Jet Propulsion Laboratory, California Institute of Technology
Pasadena, California

and

N. S. Cohen
Cohen Professional Services
Redlands, California

ABSTRACT

Two different independent variable forms, a difference form and ratio form, were investigated for correlating the normalized magnitude of the measured erosive burning rate augmentation above the threshold, r/r_o, in terms of the amount that the driving parameter (mass flux or Reynolds No.) exceeds the threshold value for erosive augmentation at the test condition. The latter was calculated from the previously determined threshold correlation. Either variable form provided a correlation for each of the two motor size data bases individually. However, the data showed a motor size effect, supporting the general observation that the magnitude of erosive burning rate augmentation is reduced for larger rocket motors. For both independent variable forms, the required motor size scaling was attained by including the motor port radius raised to a power in the independent parameter. A boundary layer theory analysis confirmed the experimental finding, but showed that the magnitude of the scale effect is itself dependent upon scale, tending to diminish with increasing motor size.

INTRODUCTION

In the design and development of the Advanced Solid Rocket Motor (ASRM) for the NASA Space Shuttle, one of the objectives is that the new propellant's erosive burning rate characteristics should not exceed those of the current Redesigned Solid Rocket Motor (RSRM) propellant. Possible methods for making such a comparison have been investigated.

A study was previously carried out with the objective of developing a criterion for the scaling to larger rocket motor sizes of the transition or threshold conditions for erosive burning rate augmentation.[1-4] A series of rocket test firings were carried out, systematically varying the parameters considered to control the phenomenon: (1) motor port diameter, (2) length-to-diameter ratio, (3) crossflow velocity, (4) chamber pressure, (5) propellant non-erosive (base) burning rate, and (6) propellant surface roughness.

The base-line propellant formulation was the nominal Shuttle solid rocket motor formulation as manufactured by JPL -- 70% ammonium perchlorate (AP) oxidizer (70/30 coarse-fine bimodal blend) and Fe_2O_3 burning rate catalyst, 15% polybutadiene acrylonitrile (PBAN) binder-fuel, and 16% aluminum. Base-line propellant burning rate and chamber pressure conditions were 0.79 cm/s (0.31 in./s) and 5.25 MPa (750 Psia), respectively.

Two motor sizes were used in the study -- (1) 0.303 m (12 in.) I.D., 0.51 m (20 in.) long Ballistics and Test Evaluation System (BATES) motor chambers and (2) 0.127 m (5 in.) I.D., 0.254 m (10 in.) long (5 x 10) batch check motor chambers -- bolted together as segments, Figs. 1 and 2. The motors were instrumented at several locations along their length with pressure transducers and plasma capacitance gauges (PCG's) -- an instrument for continuously measuring the propellant burning rate. Each PCG consists of a capacitor formed between an electrode located at the outer surface of the propellant grain and the ionized flame zone, with the propellant web as the capacitor dielectric. The changing capacitance with regression of the burning surface yields a continuous measurement with time of the local propellant web thickness and consequently burning rate.

TEST RESULTS

The results for the motor tests were documented in Refs. 1-4. Fig. 3 is a plot of the mean pressure at the axial measurement stations along the motor for a typical 5 x 10 segmented motor test, showing the higher than predicted pressure caused by the erosive burning-rate augmentation. Typical burning rate results, normalized by the no-crossflow, base burning rates at the corresponding test

---

*The research described in this paper was carried out at the Jet Propulsion Laboratory, California Institute of Technology, under contract with the National Aeronautics and Space Administration.

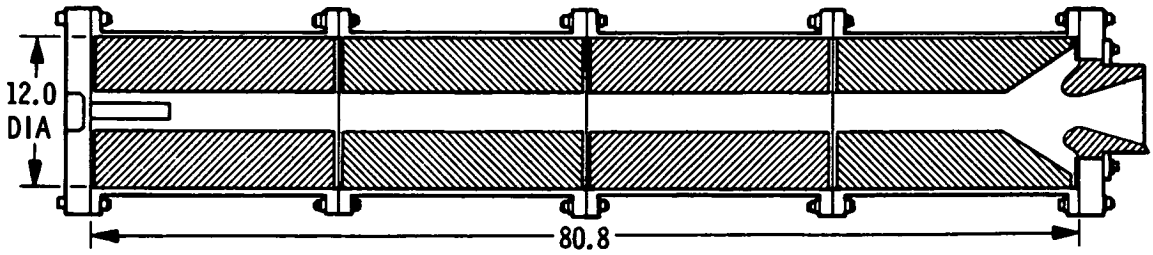

Fig. 1. BATES Erosive Burning Test Motor

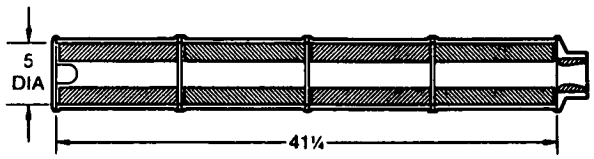

Fig. 2. Segmented 5x10 in. Batch-Check Motor Chambers

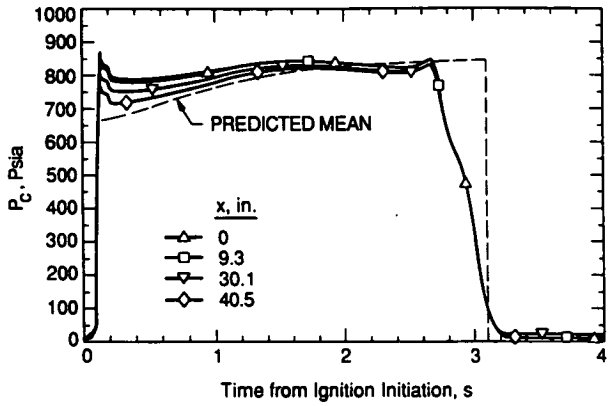

Fig. 3. Measured Chamber Pressure and Predicted Mean Pressure (No Erosion) vs. Time, Four Segment Test

pressures, are plotted in Figs. 4 and 5 for a four- and five-segment 5 x 10 motor test, respectively. The key points of information are the motor conditions at the erosive augmentation threshold (where r/r_o goes to unity) and the magnitudes of the burning rate augmentation above the threshold.

THRESHOLD CORRELATION

The threshold conditions, where the burning rate levels off at its non-erosive value, have been correlated, Fig. 6, by an expression of the form[2,3]

$$Re_c = K(L/R)\ R\acute{e}_s \tag{1}$$

where Re_c is the critical crossflow Reynolds No.

$$Re_c = \frac{\rho\ u_\infty R}{\mu_\infty} \tag{2}$$

and $R\acute{e}_s$ is a reduced surface transpiration (burning rate) Reynolds No.

$$R\acute{e}_s = \phi\ \frac{\rho_p rR}{\mu_s} \tag{3}$$

The form of the correlation was suggested by an analysis of Beddini,[5] in which the ability of the core flow turbulence to penetrate the combustion zone in the presence of blowing was evaluated. Beddini's result was modified to include a length to radius (or diameter) dependence that was displayed by these motor data.

The parameter ϕ is a function of the ratio of propellant surface temperature to core flow gas temperature.[5] A value of 0.06 was used in constructing the Eqn. (1) correlation.

EROSIVE AUGMENTATION MAGNITUDE

In the current study several methods for comparing the erosively augmented burning characteristics of propellants have been investigated, using the previously described database.

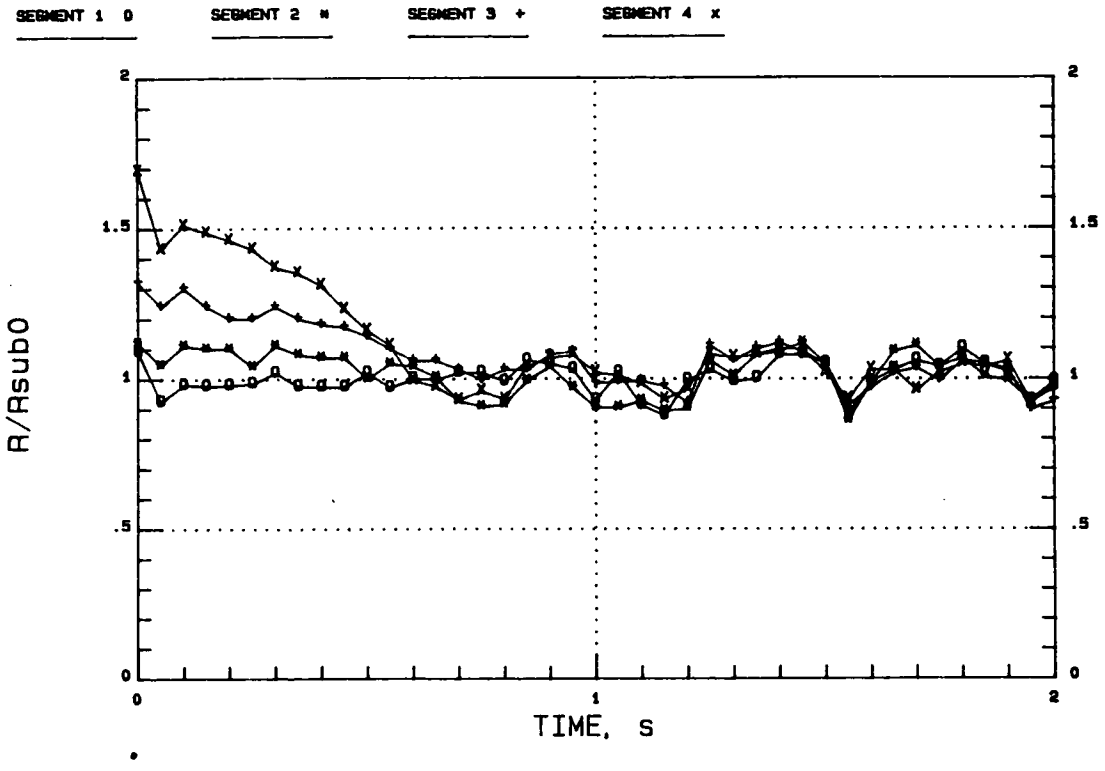

Fig. 4. Burning Rate Augmentation vs. Time, Four Segment Test

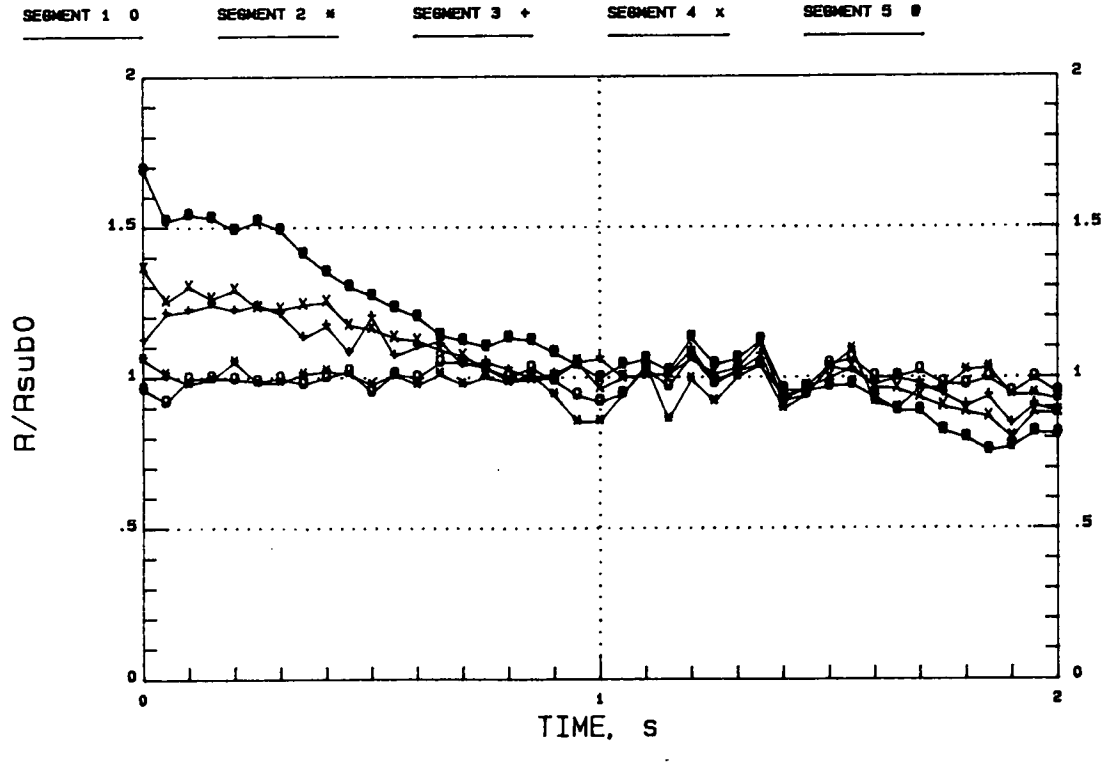

Fig. 5. Burning Rate Augmentation vs. Time, Five Segment Test

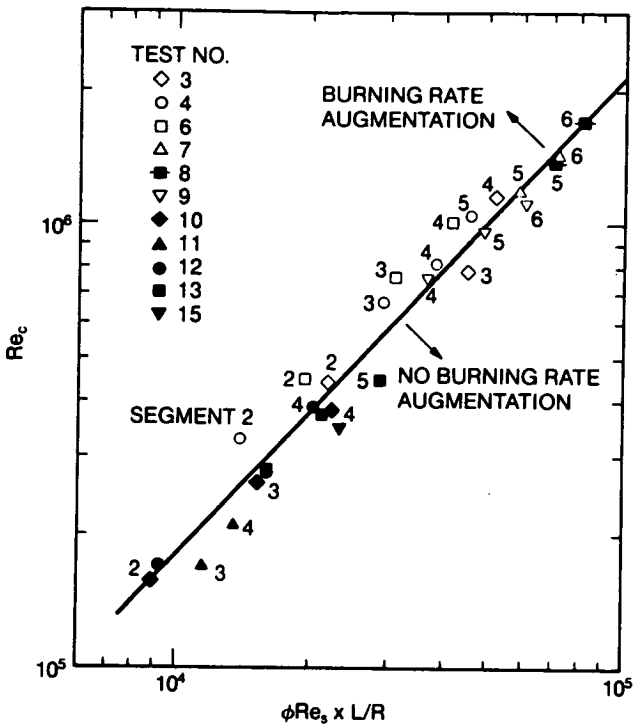

Fig. 6. Radius-Based Crossflow Reynolds No. vs. Length-Based Reduced Surface-Transpiration Reynolds No. for Erosive Burning Transition

The concept of correlating the burning rate augmentation magnitude by the amount that the driving parameter exceeds an erosive threshold value has been used by earlier investigators[6] and is used in the Erosive Burning Model No. 1 in the AFRPL Nozzleless Rocket Motor Internal Ballistics Computer Program. Since the crossflow Reynolds No. threshold value can be readily calculated from the Eqn. 1 correlation, using the threshold region base burning rate to calculate $\dot{R}e_s$ (by definition $r = r_o$ at the erosive threshold), Re_c was initially investigated as the erosive augmentation driving parameter. In Fig. 7 the burning rate augmentation results for the segmented 5 x 10 motor tests are plotted versus the amount Re_c exceeds the erosive threshold value.

When the segmented BATES motor test results are added, Fig. 8, a distinct size scaling effect is apparent. Therefore, the motor port radius raised to a negative power was added to the independent parameter. A curve fit analysis yielded a best fit value of -2.4 (chi-square = 0.0389) for the exponent, Fig. 9. The Re_c values are also raised to the 0.8 power, as suggested by correlations for convective heat transfer to the surface in turbulent pipe flow.

The ratio of Re_c and $Re_{c,th}$ produced a poorer correlation, but the variable $(Re_c/Re_{c,th}/R^{0.5})^{0.8}$ did provide the required motor size scaling, Fig. 10.

Difference and ratio forms of the mass flux, G, as the driving parameter were also investigated. Obtaining G_{th} from the Eqn. 1 correlation requires the motor port radius, in addition to the propellant base burning rate, at the threshold condition. The experimentally determined values for each test were used. For the difference form, the independent parameter $(G^{0.8} - G_{th}^{0.8})/R^{0.4}$ provided the required size scaling, Fig. 11. The dependent parameter was changed to $r/r_o - 1$ for this case. The ratio form correlation, although again poorer, showed very little size scale effect, Fig. 12.

MECHANISM FOR THE FOR THE EFFECT OF SCALE

INTRODUCTION

Many of the erosive burning models do not show an effect of scale (motor size) on the magnitude of erosive burning. The two most commonly used expressions in the solid propulsion community have been those of Lenoir & Robillard[7] and Saderholm.[8] These models were based on heat transfer from a core gas flow parallel to the propellant burning surface. The Lenoir-Robillard expression is a function of crossflow mass flux and nominal (base) propellant burn rate, but not of scale. While it does contain an explicit length-dependence, that length-dependence comes from the Chilton-Colburn equation for flow over a flat plate and is not really a scale factor in the sense of motor size (diameter). The expression has been applied to different motors by adjusting the two empirical

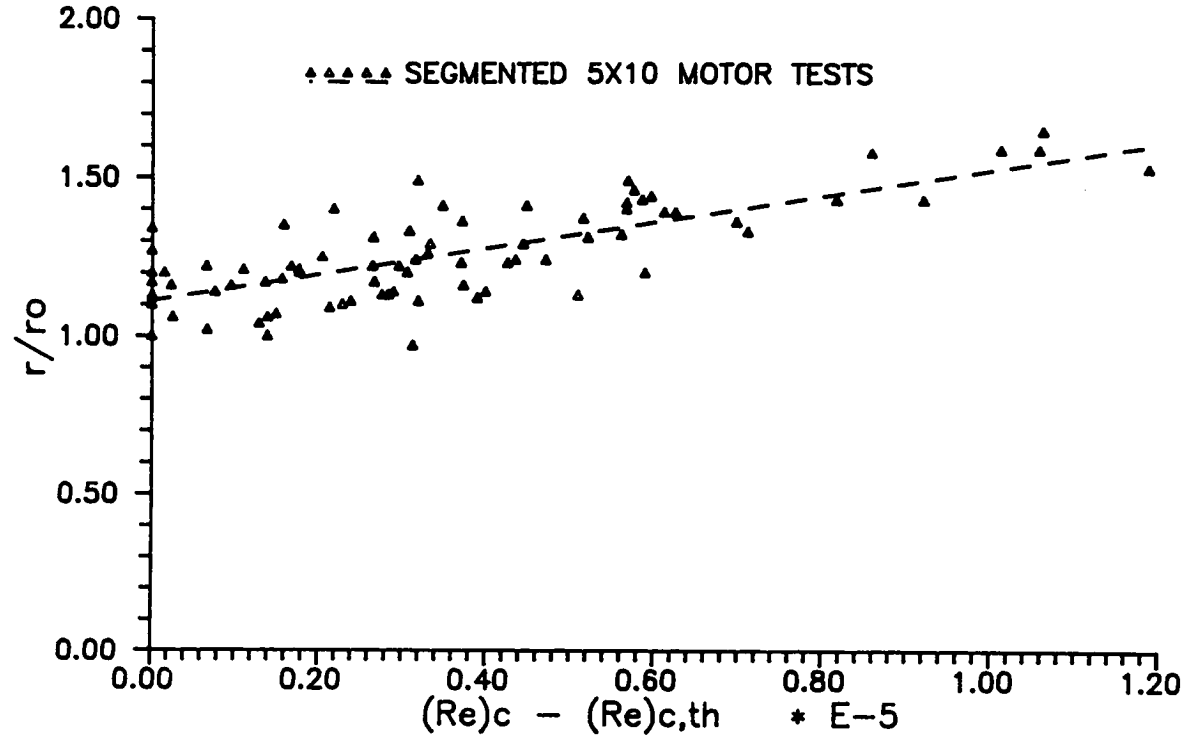

Fig. 7. Burning Rate Augmentation vs. Re No. - Re No.,th, Segmented 5x10 Motor Tests

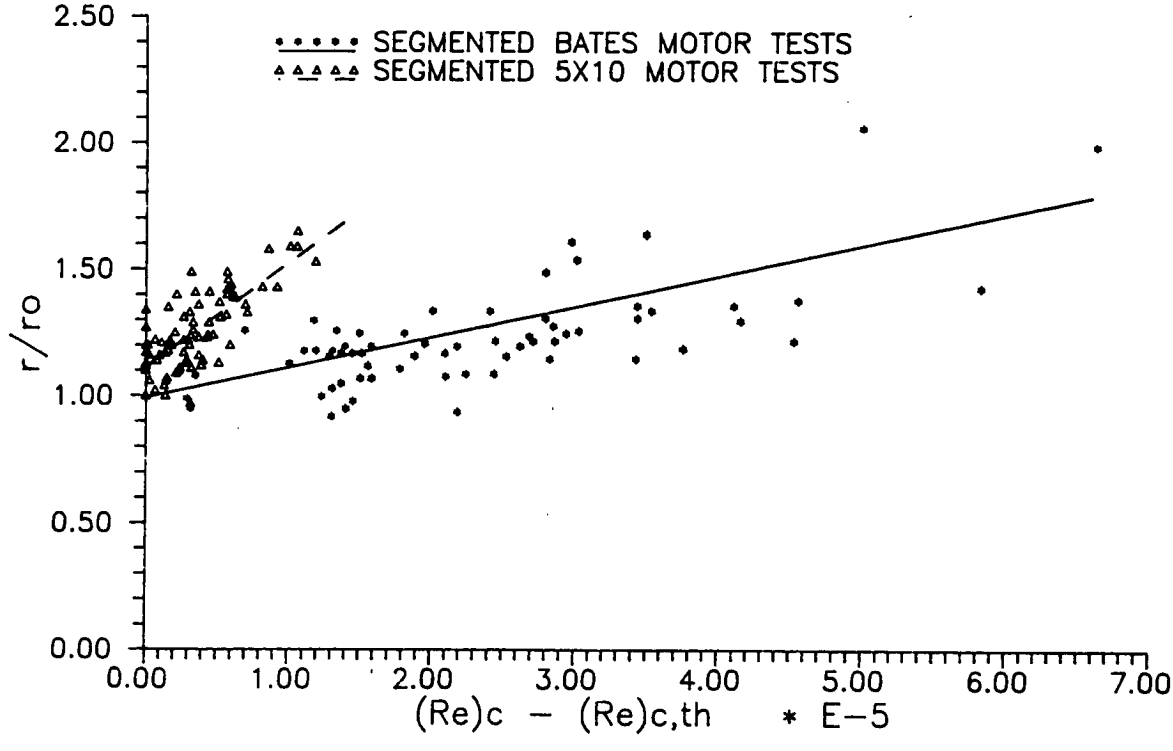

Fig. 8. Burning Rate Augmentation vs. Re No. - Re No.,th, Segmented BATES and Segmented 5x10 Motor Tests

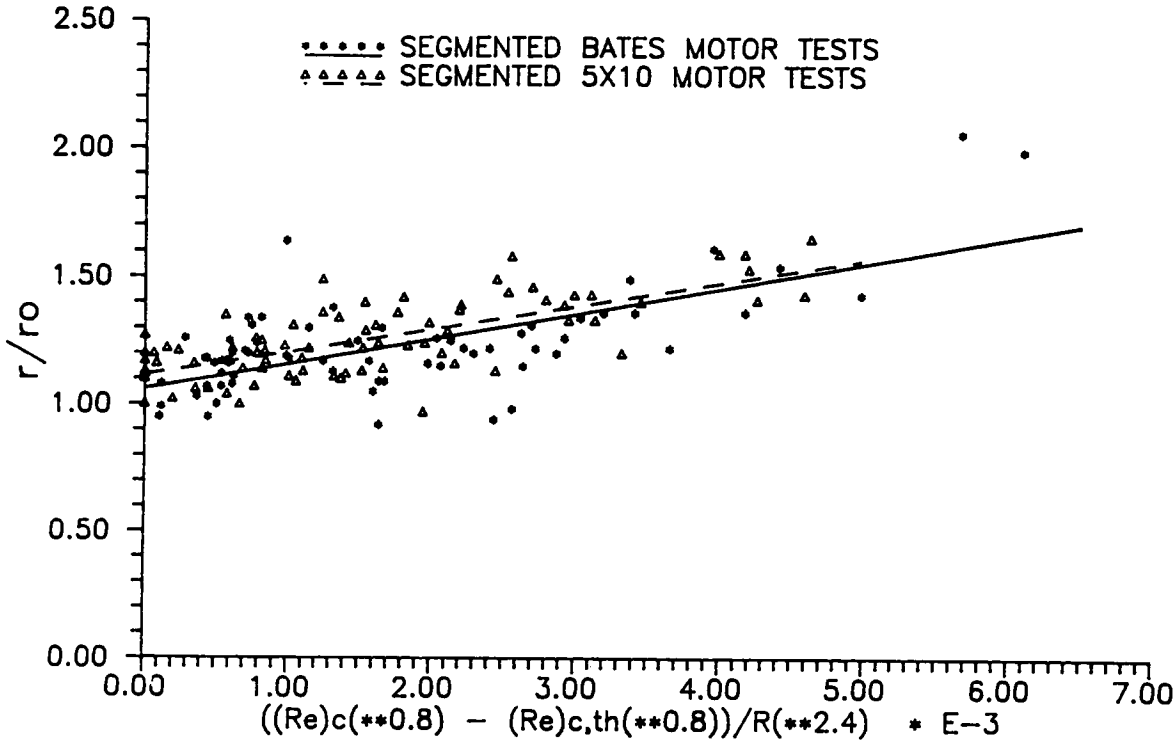

Fig. 9. Burning Rate Augmentation vs. (Re No.(**0.8) - Re No.,th(**0.8))/R(**2.4)

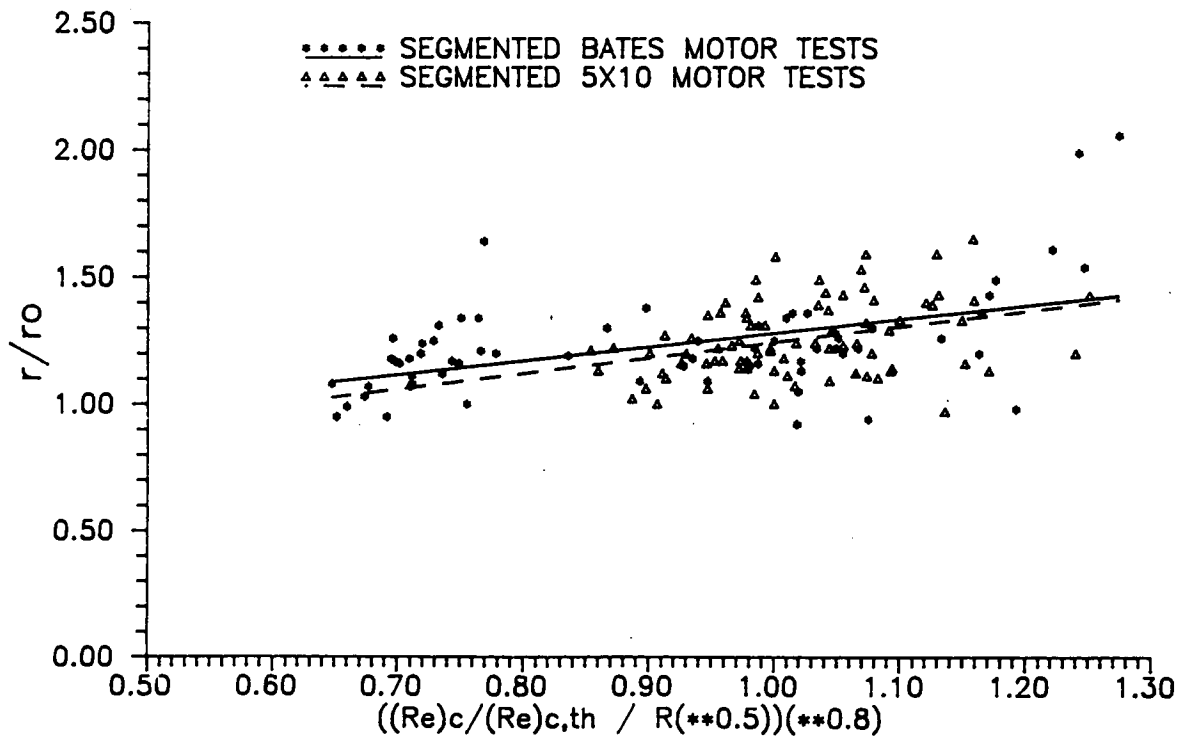

Fig. 10. Burning Rate Augmentation vs. (Re No./Re No.,th/R(**0.5))(**0.8)

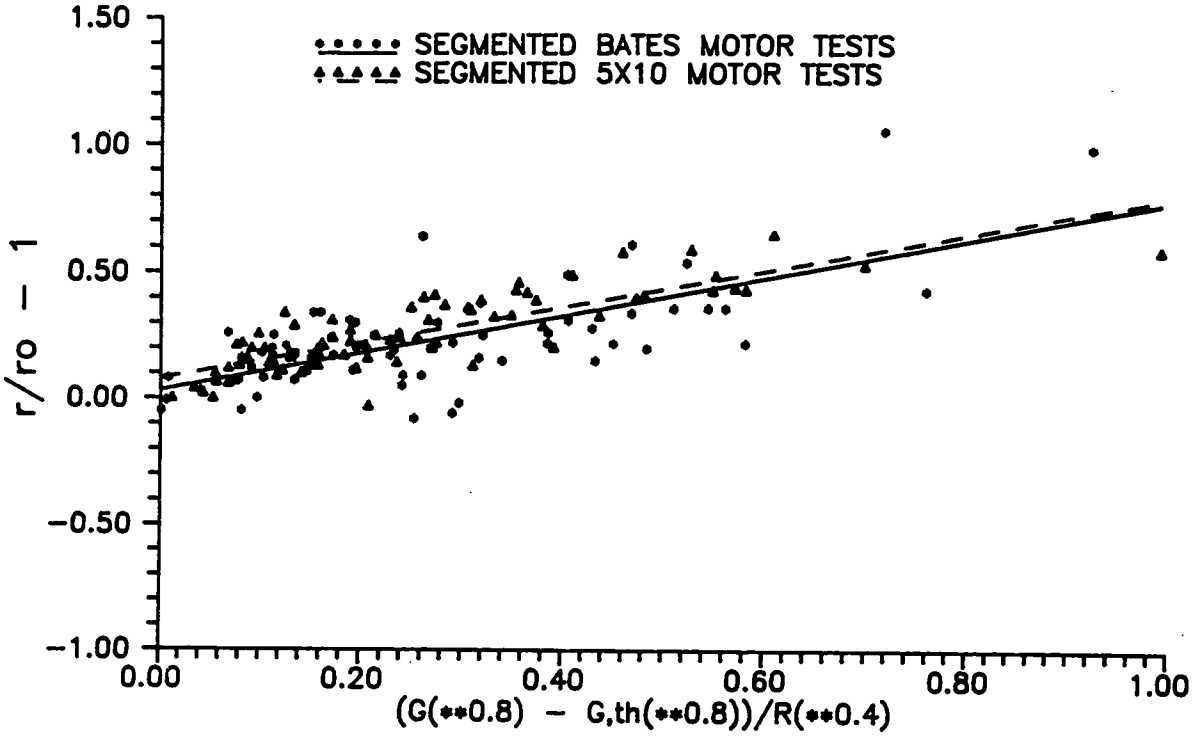

Fig. 11. Burning Rate Augmentation vs. (G(**0.8) - G,th(**0.8))/R(**0.4)

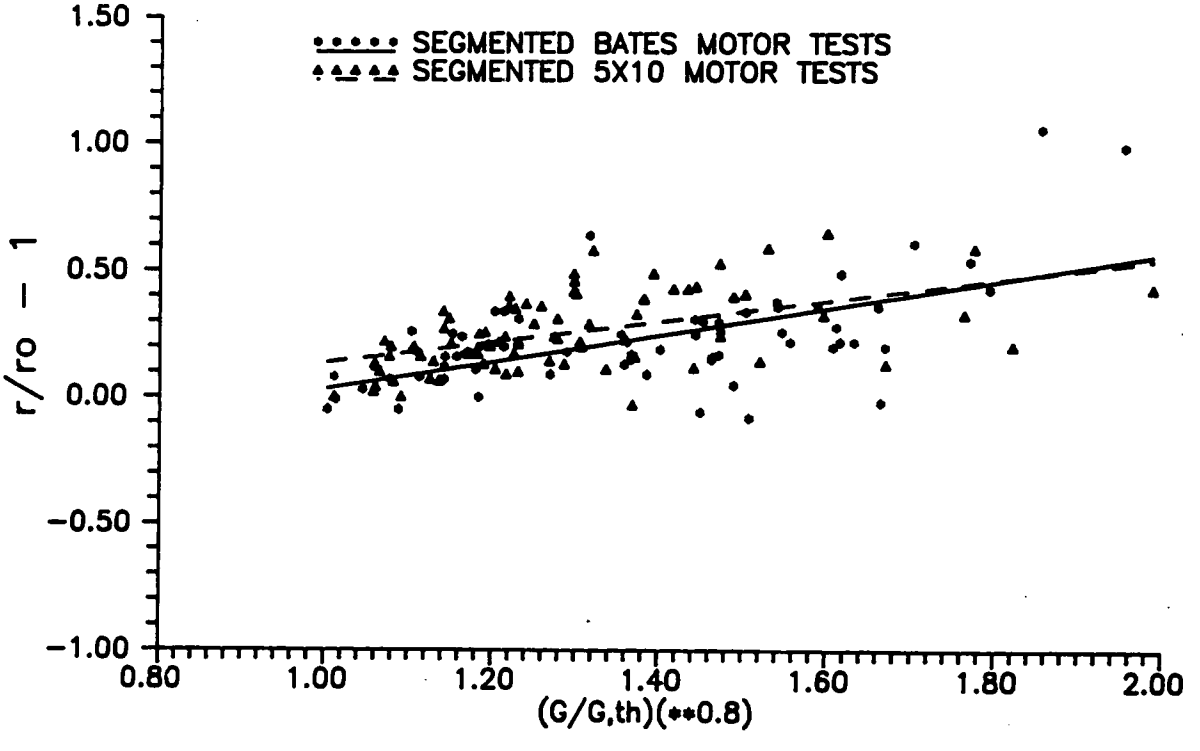

Fig. 12. Burning Rate Augmentation vs. (G/G,th)(**0.8)

constants that it contains. Saderholm's expression boils down to an empirical correlation with crossflow velocity, pressure and base burn rate, and may similarly be adjusted (fitted) to different motors. While these expressions have shown correct functional dependencies, the needed adjustments render them inadequate to design new large motors such as proposed advanced solid rocket boosters.

Some of the more sophisticated models of erosive burning have shown an effect of scale.[6,9,10] The effect is not obvious from the system of equations, but has been shown in calculated results. There are other models which contain this effect of scale, but they were not applied to show it.[11-13] Results which have been obtained show a decrease in erosive burning with increasing scale.

One can readily verify that a scaled-up motor has the same core gas flow velocity and mass flux as its geometrically identical subscale counterpart when operating at the same pressure. Thus the effect of scale cannot be related to dependencies on velocity or mass flux. Using diameter as the scale factor, the core Reynolds number varies directly with scale and the mass flow rate varies directly with the square of scale. Thus the Reynolds number per se, or the mass flow rate, cannot be a basis for an effect of scale which diminishes erosive burning. On the other hand, the axial pressure gradient in the motor varies inversely with scale and is of mechanistic significance in boundary layer theory.[9,14,15] Another relevant parameter that varies inversely with scale is combustion zone thickness as a fraction of port radius or boundary layer thickness.

ANALYSIS

The following analysis is meant to illustrate the effect of scale in a mechanistic sense. Equations are simplified to the extent possible so that the forest is not lost for the trees. Where calculated results are presented, the proper complete equations were used.

An important starting parameter is the wall shear stress, given by:

$$\tau_w = \rho_\infty u_\infty^2 (C_f/2) \tag{4}$$

The friction coefficient in the presence of wall transpiration (blowing) may be related to the value in the absence of blowing by (e.g., Ref. 14):

$$C_f/C_{fo} = \exp\left[-\frac{K_1 \rho_p r}{\rho_\infty u_\infty C_{fo}}\right] \tag{5}$$

and a simple expression for C_{fo} may be written as:[14]

$$C_{fo} = K_2/Re^{0.13} \tag{6}$$

Recognizing that a rocket motor is a self-contained, mass-generating system, the core velocity can be expressed in terms of Reynolds number by the definition of Reynolds number. In other words, a rocket motor is not a laboratory burner experiment wherein velocity can be varied independently by external means. Then combing these equations yields:

$$\tau_w = \frac{K_3 \mu_\infty^2/\rho_\infty}{(D^2/Re^{1.87}) \exp(K_4 D/Re^{0.87})} \tag{7}$$

It is observed that there is an effect of diameter distinct from that of Reynolds number. Moreover, it is clear that increasing motor size (noting that Re ~ D) decreases the wall shear stress. For a given motor size, increasing Re by increasing u_∞ (downstream L/D locations) increases the wall shear stress. These effects are illustrated in Fig. 13, but using Koo's complete expression for C_{fo}.[16] This mechanism is a result of the axial pressure gradient in the motor.

The diameters selected for Fig. 13 represent the two subscale motors used in this study and the Space Shuttle solid rocket motor (SRM). These are initial port diameters, inasmuch as erosive burning is largest at that time.

One class of erosive burning combustion models is based upon turbulence-enhanced transport properties in the combustion zone.[12,14] The enhancement is related to the turbulence momentum diffusivity by:

$$t \sim 1 + (\rho\epsilon)/\mu \tag{8}$$

which, in turn, is related to the local shear stress:

$$1 + (\rho\epsilon)/\mu = \tau/(\mu du/dy) \tag{9}$$

The augmented transport properties are computed by solving for the velocity profile in the combustion zone near the propellant surface. The relation for the eddy viscosity is:

$$\epsilon = K_5 y^2 du/dy \tag{10}$$

To simplify the solution procedure, King[14] used a momentum integral analysis to describe the local shear stress:

$$\tau = \tau_w + \rho_p r\, u_\infty [(u/u_\infty) - K_6(y/D)] \tag{11}$$

Equating (9) and (11) for τ, using (10) for ϵ and using (7) for τ_w, provide the required differential equation for du/dy. To bring in Reynolds number and motor diameter, it is convenient to non-dimensionalize u by u_∞ and y by D as suggested from Eq. (11). For purposes of making calculations, it is also necessary to account for changes in local gas density and viscosity with temperature; but that will be omitted from the equations for the sake of clarity. The result of these manipulations is:

$$du'/dy' = (-B + \sqrt{B^2 - 4AC})/2 \tag{12}$$

$$\text{where} \quad A = K_5\, Re\, y'^2 \tag{12a}$$

$$B = 1 \tag{12b}$$

$$-C = \frac{K_3 Re^{0.87}}{\exp(K_4 D/Re^{0.87})} + \frac{\rho_p r D}{\mu}(u' - K_6 y') \tag{12c}$$

It is observed that diameter appears distinct from Reynolds number in several places. It appears in A, as the dimensionless y. In other words, the larger the motor, the lower the value of y' for a fixed combustion zone thickness (fixed mainly by propellant formulation and pressure). Thus the combustion zone "sees" a lower velocity gradient and shear stress. It also appears in C, expressing effects of axial pressure gradient with blowing. However, the effects in C are conflicting. In the first term, which comes from the wall shear stress, increasing D tends to reduce the velocity gradient (reduce the shear stress) at the wall. In the second term, which comes from momentum conservation, increasing D has the opposite effect away from the wall. For combinations of high Reynolds numbers and low propellant burn rates, the first term dominates within the combustion zone so that increasing D clearly tends to reduce turbulence enhancement. Under those conditions, the velocity gradient in the combustion zone may be obtained without numerical integration. On the other hand, King has noted difficulties with this approach at high burning rates where the second term becomes larger.[14]

In performing the numerical integration for the velocity gradient, care must be exercised in treating the region immediately adjacent to the wall (see, e.g., Ref. 17). Knowing the velocity gradient as a function of y', the shear stress and the augmentation factor are also known as functions of y'. The combustion models[12,14] then use averaged augmentation values appropriate to various flame heights. For purposes of this study, a constant flame height of 100 μm was assumed to set the basis for y'. Calculated values of augmentation factor were averaged over this distance for each case.

DISCUSSION OF RESULTS

Results of calculations of augmentation factor for the conditions corresponding to Fig. 13 are shown in Fig. 14. The abscissa has been changed in order to comport with the data correlation plot (Fig. 9) and examine the effect of port radius in that context. Several items of interest are apparent from Figure 14.

First, it is clear that effects of scale on augmentation factor are not nearly as large as on wall shear stress. While variations in Reynolds number produce changes of many orders of magnitude in τ_w, the changes in t are within an order of magnitude. The same holds true for variations in size at a fixed Reynolds number. Keeping the fixed L/D position in the motor with increasing motor size, the decrease in τ_w is more than an order of magnitude, but the decrease in t is well within a factor of 2. The reason for this mitigation is evident from Eq. (9): τ and du/dy both increase or decrease together with variations in the scale parameters, whereas τ_w is by itself in Eq. (7).

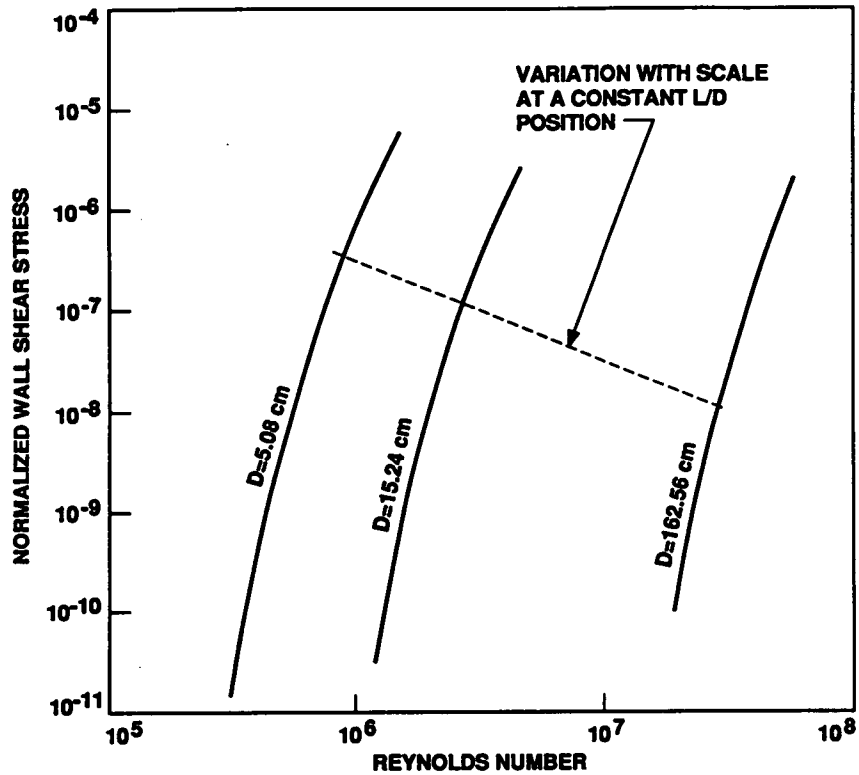

Fig. 13. Calculated Effect of Scale Parameters on Wall Shear Stress

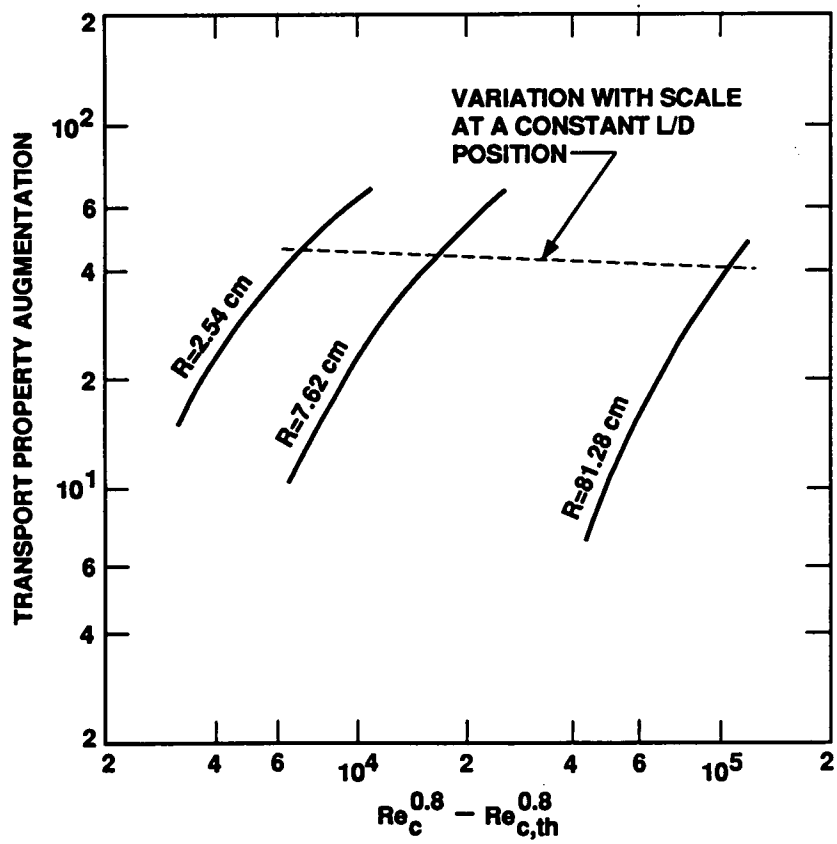

Fig. 14. Calculated Effect of Scale Parameters on Transport-Property Augmentation That Would Be Used in Erosive Burning Combustion Models

Second, it is clear that the distinct effect of diameter or radius depends upon both diameter and Reynolds number. From the correlation of data in Fig. 9, it might be thought that $R^{-2.4}$ is a general representation of the effect of radius. According to Fig. 14, this is not correct. For example, at an abscissa value of 6500, the ratio between the results for R = 2.54 cm. and R = 7.62 cm. may be expressed as $R^{-1.4}$; at an abscissa value of 10500, the ratio becomes $R^{-0.9}$. Given the uncertainties in the theory (as discussed by King[14]), quantitative discrepancies between theory and experiment are not too disturbing. However, the qualitative discrepancy (R to a variable power instead of a constant power) is considered to be important.

Third, a curvature is noted in the Figure 14 results. Indeed, it might be speculated that the curves will merge at very high Reynolds numbers. This curvature is responsible for the variable R-dependence. Accordingly, the equations were analyzed for the limiting conditions of infinite Reynolds number and zero Reynolds number. One can verify that, at infinite Reynolds number, the augmentation factor becomes proportional to Reynolds number and independent of radius. Thus the R-dependence goes away (curves will merge) at very high Reynolds number. The zero Reynolds number limit is a trivial case, and the equations do show the augmentation going to 1.0 as the Reynolds number goes to zero. Again, the R-dependence vanishes. It would therefore appear that the R-dependence maximizes under conditions near erosive thresholds, as captured in Figure 14, and goes away at Reynolds number extremes. This is important because it suggests that a reasonably economical subscale test motor (e.g., Super-BATES motors) would closely represent an SRM-size motor.

Fourth, the change in augmentation factor with scale seems to be small for a constant L/D position in the motor. The authors have no experience in relating changes in t to changes in burn rate because their erosive combustion model is based upon a different approach.[18] Perhaps some future work can close this loop. For now, suffice it to say that calculated theoretical effects of scale on erosive burning rate that have appeared in the literature are small for baseline conditions of interest.

CONCLUSIONS

The measured magnitude of erosive burning rate augmentation was correlated by the amount that the driving parameter (mass flux or Reynolds number) exceeds the threshold value for erosive augmentation at the test condition. However, the data exhibited a motor size effect, the magnitude of burning rate augmentation decreasing with increasing motor size (scale).

Application of boundary layer theory confirms the experimental finding, but shows that the scale effect is itself dependent upon scale, tending to diminish with increasing motor size. The useful implication of this theoretical result is that a large subscale motor would be closely representative of SRM-class solid boosters, whereas a small or standard subscale motor would not be.

The mechanisms for this effect of scale are the reduction in axial pressure gradient in the empiricisms of boundary layer theory, and the reduction in combustion zone thickness relative to the boundary layer or motor. The result is a reduction in the shear stress and turbulence momentum diffusivity in the combustion zone, with attendant reduction in turbulence transport properties that affect burn rate.

NOMENCLATURE

C_f	friction coefficient with blowing
C_{fo}	friction coefficient in the absence of blowing
D	propellant grain port diameter
G	mass flux
K	constants
L	grain length
P_c	motor chamber pressure
r	propellant burning rate
r_o	no-crossflow, base burning rate
R	grain port radius
Re	Reynolds number based on radius or diameter, as defined in text

t	transport property augmentation factor; for example, ratio of thermal conductivities with and without turbulence
u	local gas velocity in the boundary layer
u'	u/u_∞
y	radial distance from the wall (propellant surface)
y'	y/D
ϵ	local eddy viscosity
μ	local gas viscosity
ρ	local gas density
ρ_p	propellant density
τ	local shear stress
τ_w	shear stress at the wall
ϕ	Beddini parameter, defined in Ref. 5

subscripts

c	crossflow
s	surface
th	threshold
∞	core flow

REFERENCES

1. Strand, L., Yang, L., Nguyen, M., and Cohen, N., "Erosive Burning Research," AIAA Paper No. 86-1449, June 1986.

2. Strand, L. D., Nguyen, M. H., and Cohen, N. S., "The Scaling of the Threshold Conditions for Solid Propellant Erosive Burning," AIAA Paper No. 88-3254, July 1988.

3. Strand, L. and Cohen, N., "Erosive Burning Threshold Conditions in Solid Rocket Motors," AIAA Paper No. 89-2528.

4. Strand, L., Yang, L., Ray, R., and Barry, J., "Erosive Burning Research," 22nd JANNAF Combustion Meeting, CPIA Publication 432, Vol. I, Chemical Propulsion Information Agency, Laurel, MD, Oct. 1985, pp. 29-40.

5. Beddini, R. A., "On the Scaling of Solid Propellant Erosive Burning: The Threshold Condition," 15th JANNAF Combustion Meeting, CPIA Publication 297, Vol. II, Chemical Propulsion Information Agency, Laurel, MD, Feb. 1979, pp. 199-216.

6. Razdan, M. K. and Kuo, K. K., "Erosive Burning of Solid Propellants," Fundamentals of Solid-Propellant Combustion, edited by K. K. Kuo and M. Summerfield, Progress in Astronautics and Aeronautics, Vol. 90, American Institute of Aeronautics and Astronautics, New York, NY, 1984, pp. 515-598.

7. Lenoir, J. M. and Robillard, G., "A Mathematical Method to Predict the Effects of Erosive Burning in Solid Propellant Rockets," Sixth Symposium (International) on Combustion, Reinhold, New York, NY, 1957, pp. 553-667.

8. Saderholm, C. A., "A Characterization of Erosive Burning for Composite Propellants," AIAA Solid Propellant Rocket Conference, Palo Alto, CA, Jan. 1964.

9. Beddini, R. A., "Reacting Turbulent Boundary Layer Approach to Solid Propellant Erosive Burning," AIAA J., Vol. 16, No. 9, Sept 1978, pp. 898-905.

10. King, M. K., "Predicted and Measured Effects of Pressure and Crossflow Velocity on Composite Propellant Burning Rate," 17th JANNAF Combustion Meeting, CPIA Publication 329, Vol. I, Chemical Propulsion Information Agency, Laurel, MD, Nov. 1980, pp. 99-122.

11. Lengelle, G., "Model Describing the Erosive Combustion and Velocity Response of Composite Propellants," AIAA J., Vol. 13, No. 3, Mar. 1975, pp. 315-322.

12. Renie, J. P. and Osborn, J. R., "Erosive Burning," AIAA J., Vol. 21, No. 12, Dec. 1983, pp. 1681-1689.

13. Godon, J. C., Duterque, J., and Lengelle, G., "Solid Propellant Erosive Burning," AIAA Paper No. 87-2031, July 1987.

14. King, M. K., "A Model of the Effects of Pressure and Crossflow Velocity on Composite Propellant Burning Rate," AIAA Paper No. 79-1171, June 1979.

15. Arora, R., Wu, K., White, F. X., and Kuo, K. K., "Erosive Burning of Composite Solid Propellants: Mechanism, Correlation, and Grain Design Applications," J. of Spacecraft and Rockets, Vol. 20, No. 1, Jan.-Feb. 1983, pp. 43-48.

16. McAdams, W. H., Heat Transmission, McGraw-Hill Series in Chemical Engineering, New York, NY, 1954, p. 155.

17. Razdan, M. K. and Kuo, K. K., "Turbulent Flow Analysis of Erosive Burning of Cylindrical Composite Solid Propellants," AIAA J., Vol. 20, No. 1, Jan. 1982, pp. 122-128.

18. Cohen, N. S. and Strand, L. D., "Effect of AP Particle Size on Combustion Response to Crossflow," AIAA J., Vol. 23, No. 5, May 1985, pp. 776-781.